

## Supporting Information

# Enhanced electrochromic and energy storage performance in mesoporous WO<sub>3</sub> film and its application in bi-functional smart window

Wei-qi Wang <sup>ab</sup>, Xiu-li Wang <sup>a\*</sup>, Xin-hui Xia <sup>a\*</sup>, Zhu-jun Yao <sup>a</sup>, Yu Zhong <sup>a</sup>, and Jiang-ping Tu <sup>ab\*</sup>

*a. State Key Laboratory of Silicon Materials, Key Laboratory of Advanced Materials and Applications for Batteries of Zhejiang Province, and School of Materials Science & Engineering, Zhejiang University, Hangzhou 310027, China*

*b. Research Institute of Zhejiang University-Taizhou, 318000, China*

\*Corresponding author. Tel: +86 571–87952856; Fax: +86 571–8792573

Email: wangxl@zju.edu.cn; helloxxh@zju.edu.cn; tujp@zju.edu.cn

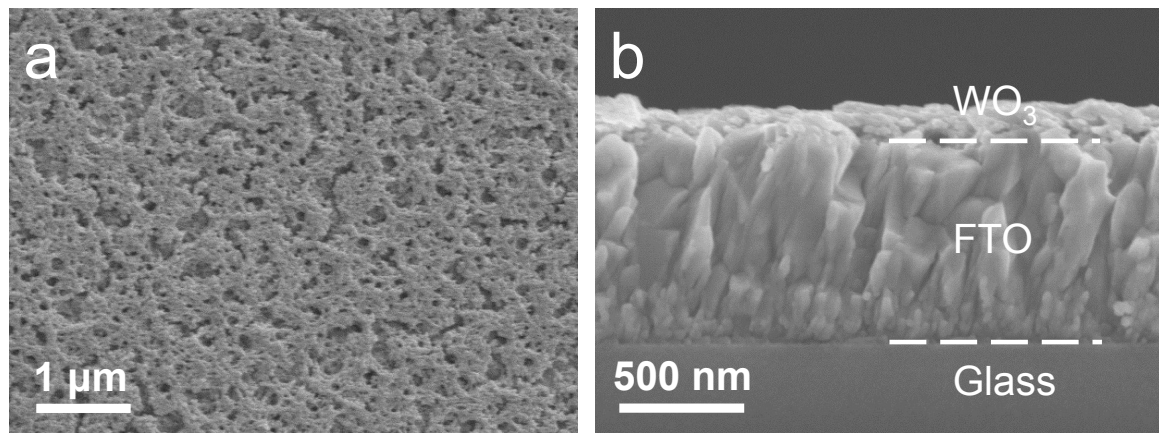


**Figure S1.** (a) SEM image and (b) cross sectional view of the macroporous  $\text{WO}_3$  thin film on FTO glass.

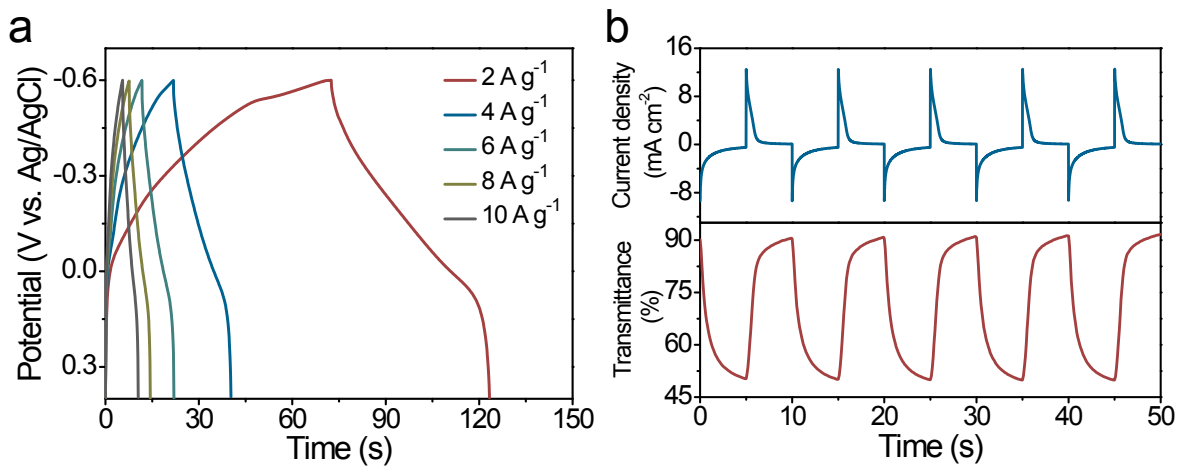


**Figure S2.** (a) Galvanostatic charge/discharge curves of the macroporous  $\text{WO}_3$  film at different current densities. (b) Chronoamperometry curve and the corresponding in situ transmittance curve at 633 nm for the macroporous  $\text{WO}_3$  film.

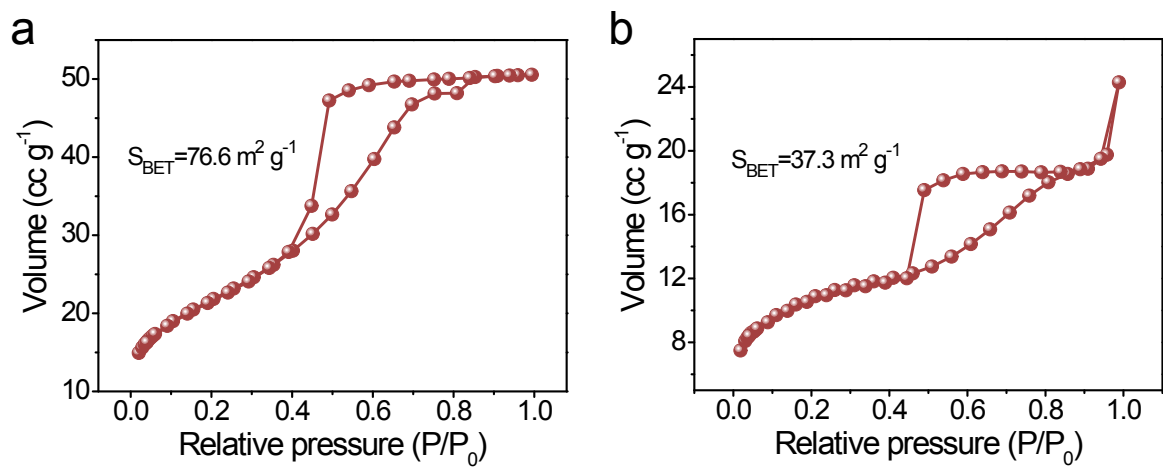


**Figure S3.** Nitrogen adsorption-desorption isotherm curve of (a) mesoporous  $\text{WO}_3$  film and (b) macroporous  $\text{WO}_3$  film.

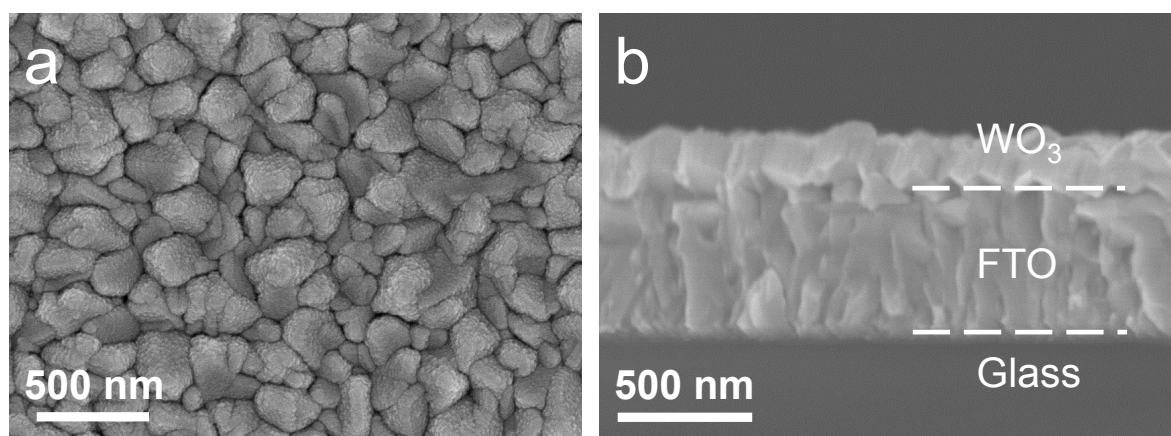


**Figure S4.** (a) SEM image and (b) cross sectional view of the dense  $\text{WO}_3$  thin film on FTO glass.

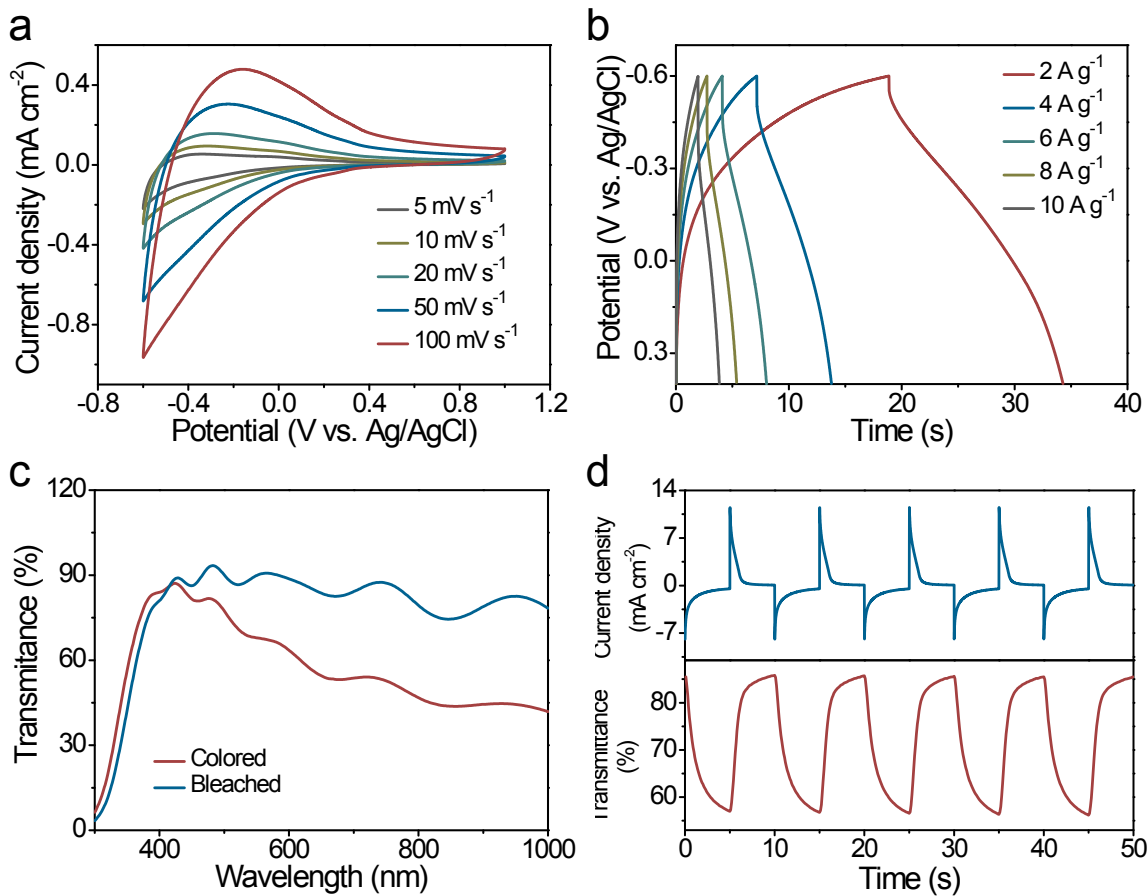


**Figure S5.** (a) CV curves of the dense  $\text{WO}_3$  film at different scan rates. (b) Galvanostatic charge/discharge curves of the dense  $\text{WO}_3$  film at different current densities. (c) Transmittance spectra of the dense  $\text{WO}_3$  film for different working states (bleached and colored). (d) Chronoamperometry curve and the corresponding in situ transmittance curve at 633 nm for the dense  $\text{WO}_3$  film.

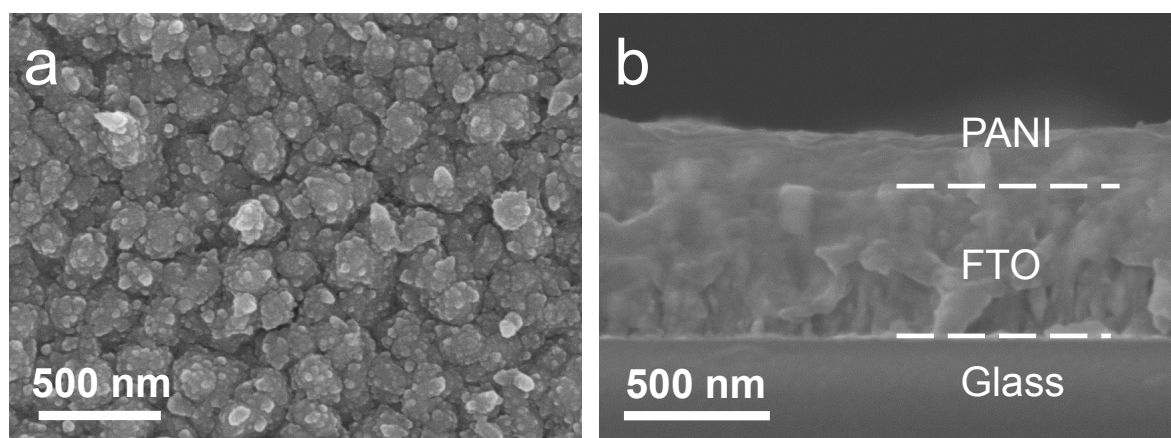


**Figure S6.** (a) SEM image and (b) cross sectional view of the PANI nanoparticles film on FTO glass.

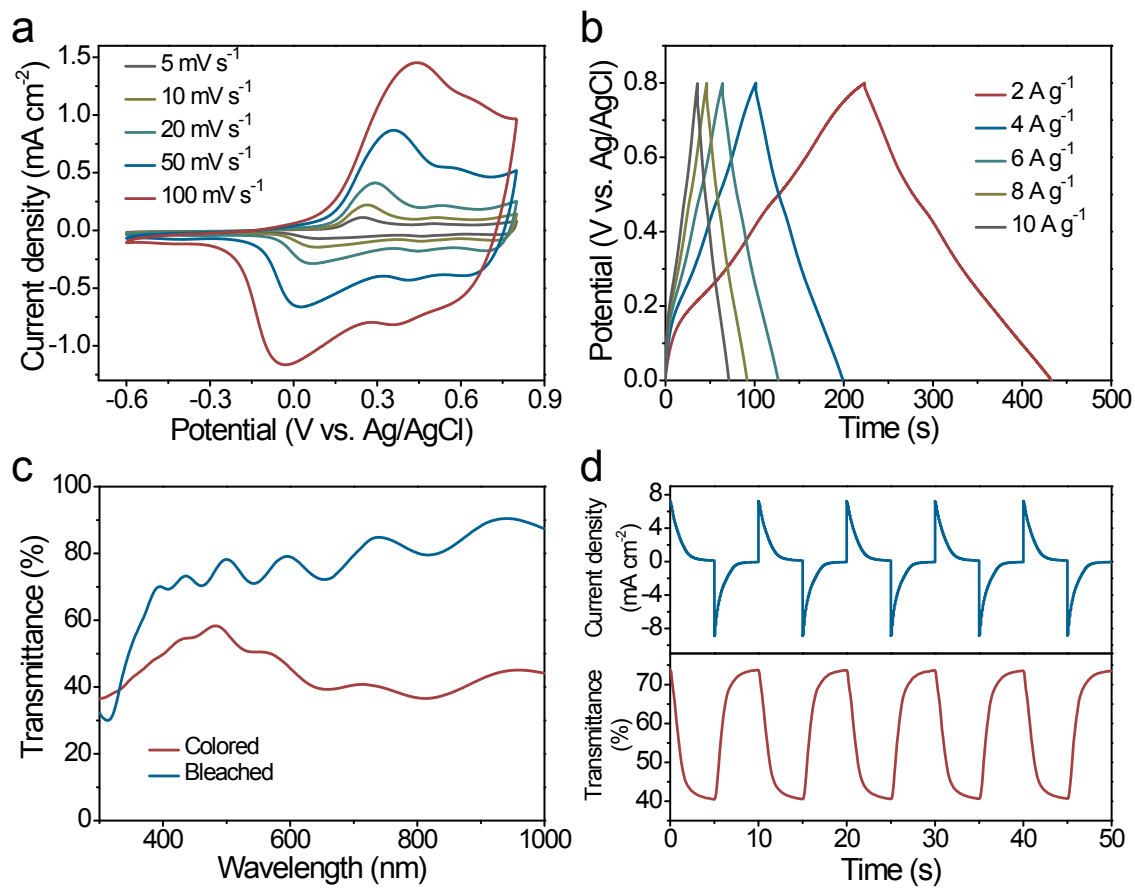


**Figure S7.** (a) CV curves of the PANI film at different scan rates. (b) Galvanostatic charge/discharge curves of the PANI film at different current densities. (c) Transmittance spectra of the PANI film for different working states (bleached and colored). (d) Chronoamperometry curve and the corresponding in situ transmittance curve at 633 nm for the PANI film.

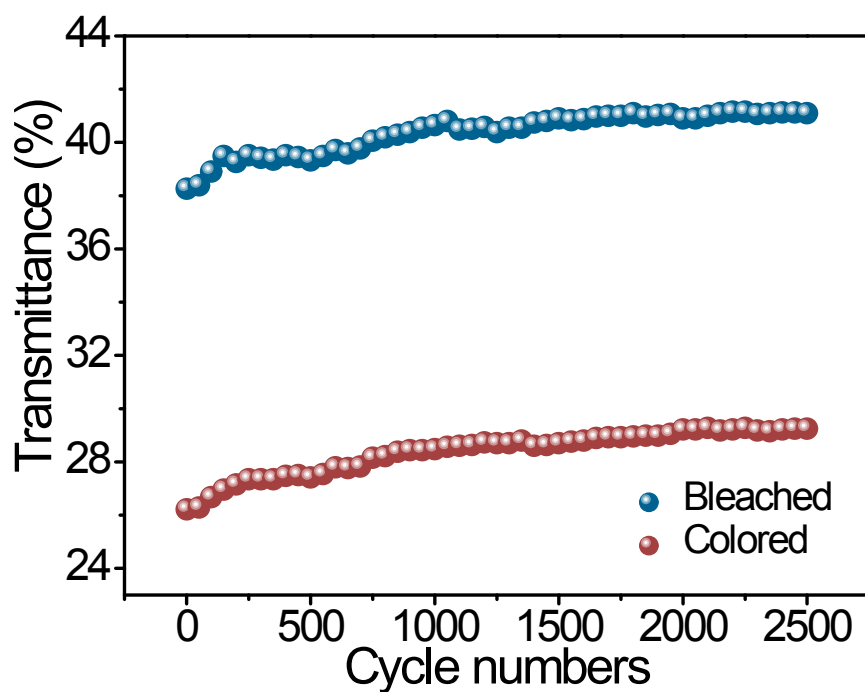


**Figure S8.** Electrochromic cyclic stability of the macroporous  $\text{WO}_3$  based device tested at 0 and 1 V for 2500 cycles.

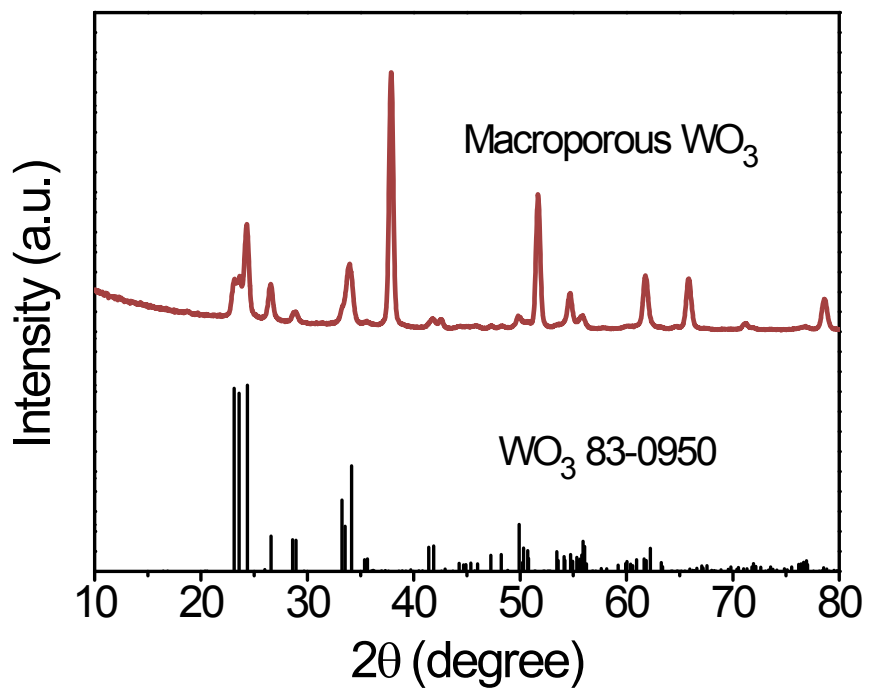


**Figure S9.** XRD patterns of the macroporous  $\text{WO}_3$  film.

**Table S1.** Transparency, optical modulation and switching speed of different morphology WO<sub>3</sub> film in the recent literatures.

Morphology	Electrolyte	Transparency (633 nm)	ΔT (633 nm)	<i>t<sub>c</sub></i> / <i>t<sub>b</sub></i> (s)	Ref.
WO <sub>3</sub> nanowire arrays	1M LiClO <sub>4</sub>	72%	58%	7.6 s/4.2 s	1
Ordered macroporous WO <sub>3</sub>	0.5M H <sub>2</sub> SO <sub>4</sub>	78%	52%	5.6 s/1.8 s	2
WO <sub>3</sub> nanoparticle	1M H <sub>2</sub> SO <sub>4</sub>	91.3%	72.6%	3.1 s/0.9 s	3
WO <sub>3</sub> nanosheet	0.5M H <sub>2</sub> SO <sub>4</sub>	72%	62%	5.2 s/2.2 s	4
WO <sub>3</sub> Quantum Dots	1M H <sub>2</sub> SO <sub>4</sub>	94%	85%	0.9 s/1.0 s	5
WO <sub>3</sub> nanoflake	1M LiClO <sub>4</sub> / PC	70%	68%	9.3 s/5.7 s	6
WO <sub>3</sub> nanoplate	0.5M H <sub>2</sub> SO <sub>4</sub>	—	38%	4.3 s/1.4 s	7
WO <sub>3</sub> nanoporous network (0.2 μm thick)	0.1M H <sub>2</sub> SO <sub>4</sub>	98% (650nm)	20% (650nm)	9.8 s/3.9 s	8
Amorphous WO <sub>3</sub>	0.5M HCl	83% (550nm)	75% (550 nm)	9.8 s/3.0 s	9
Mesoporous WO <sub>3</sub>	0.5M H <sub>2</sub> SO <sub>4</sub>	99.5%	75.6%	2.4 s/1.2 s	Our work

## References

1. J. Zhang, J. P. Tu, X. H. Xia, X. L. Wang and C. D. Gu, *J. Mater. Chem.*, 2011, **21**, 5492-5498.
2. J. Zhang, J. P. Tu, G. F. Cai, G. H. Du, X. L. Wang and P. C. Liu, *Electrochim. Acta*, 2013, **99**, 1-8.
3. P. H. Yang, P. Sun, Z. S. Chai, L. H. Huang, X. Cai, S. Z. Tan, J. H. Song and W. J. Mai, *Angew. Chem. Int. Ed.*, 2014, **53**, 11935-11939.

4. G. F. Cai, J. p. Tu, D. Zhou, L. Li, J. H. Zhang, X. L. Wang and C. D. Gu, *CrystEngComm*, 2014, **16**, 6866-6872.
5. S. Cong, Y. Y. Tian, Q. W. Li, Z. G. Zhao and F. X. Geng, *Adv. Mater.* , 2014, **26**, 4260-4267.
6. D. Y. Ma, H. Z. Wang, Q. H. Zhang and Y. G. Li, *J. Mater. Chem.*, 2012, **22**, 16633-16639.
7. Z. Jiao, X. Wang, J. Wang, L. Ke, H. V. Demir, T. W. Koh and X. W. Sun, *Chem. Commun.* , 2012, **48**, 365-367.
8. J. Z. Ou, S. Balendhran, M. R. Field, D. G. McCulloch, A. S. Zoolfakar, R. A. Rani, S. Zhuiykov, A. P. O'Mullane and K. Kalantar-Zadeh, *Nanoscale*, 2012, **4**, 5980-5988.
9. A. Subrahmanyam and A. Karuppasamy, *Sol. Energy Mater. Sol. Cells*, 2007, **91**, 266-274.